Compression and Stress Relaxation Characteristics of Alfalfa during Rotary Compression

Jiajia Fang, Haijun Li, Jian Wang, Mingshao Yang, Zeying Zong, and Yong Zhang *

In order to reduce the power consumption of the round baler and improve the quality of the bale, the compression and relaxation characteristics of alfalfa were investigated with respect to moisture content, feeding speed, and steel roll speed. Experimental trials were performed by using a steel-roll fixed chamber round baler rotary compression test platform. Three moisture contents were prepared, 18%, 21%, and 24%. The feeding speeds were set at 1.11 m·s^{-1}, 1.39 m·s^{-1}, and 1.67 m·s^{-1}, and the steel roll speeds were 106 r·min^{-1}, 126 r·min^{-1}, and 146r·min^{-1}, respectively. The experimental data for these trails were collected and three compression models and a generalized Maxwell model were fitted to the pressure, density, or time data. The maximum compression pressure decreased with the increase of moisture content and increased with the increase of feeding speed, while the steel roll speed had no significant effect on the maximum compression pressure. The stress relaxation time decreased with the increase of moisture content, feeding speed and steel roll speed. The equilibrium stress decreased with the increase of the steel roll speed and moisture content and increased with the increase of the feeding speed. All compression models had a good fit for the experimental data.

Keywords: *Compression characteristics; Stress relaxation; Alfalfa; Large round baler; Rotary compression*

*Contact information: College of Mechanical & Electrical Engineering, Inner Mongolia Agricultural University, Huhhot, 010018, P. R. China; *Corresponding author: zynmg@imau.edu.cn*

INTRODUCTION

Alfalfa stems exhibit different behavior under different compression conditions and material characteristics. Studying its compression and stress relaxation characteristics has an important impact on reducing the power consumption of round balers and improving the quality of bales (Adapa *et al.* 2002, 2009; Yan 2004; Hu and Lei 2009).

Researchers have conducted numerous studies related to the compression and stress relaxation characteristics of alfalfa straw, crop straw, and other agricultural fiber materials. Mani *et al.* (2002) studied the effect of grind size on pellet quality and concluded that a reduction in hammer mill screen size from 3.2 to 0.6 mm can result in an increase in pellet density from 5% to 16%, since finer grinds can absorb moisture than large particles. Many studies have indicated that the production of high quality pellets is possible only if the moisture content of the feed is between 8 and 12% (Sokhansanj *et al.* 2005; Mani and Sokhansanj 2006). Water both acts a binding agents and a lubricant (Mani *et al.* 2003). Holding times are most significant in reducing the effect of ‘spring-back’. The density of cubes increased by more than 5% when the holding time increased from 10 to 30 s reported by (Adapa *et al.* 2005). Watts and Bilanski (1991) showed that an increase in moisture content significantly reduced the maximum stress and the loading rate did not have any effect on the maximum stress.

However, the above-mentioned research was mainly based on the compression mechanism of a square baler, which has provided the basis for an optimized design of compression engineering. The compression model of a round baler is different from the open and closed compression model of a square baler, which encompasses rotary compression. Straw materials are subjected to a continuous load while being rolled during the compression process. It is not practical to apply the same conclusions obtained from a square baler to a round baler to optimize design. In recent years, Chinese investigators have performed compression tests on straw materials under rotary compression using a steel-roll round baler (Li 2012; Lei 2015).

These studies used chopped corn stalks, or whole rice straw stalks, for the optimal design of a round baler; however, studies have yet to be conducted using alfalfa. Furthermore, earlier studies were based on a small round baler (diameter less than 1 m). However, in the modern market, the round baling machine is generally a large round baler processing 5 to 10 $t \cdot h^{-1}$. The diameter of the produced hay bales is 1.2 to 1.8 m with a density of 100 to 120 $kg \cdot m^{-3}$ and a mass of 150 to 400 kg.

In addition, the number of compression and stress relaxation models has been developed to relate to the compaction behavior of the materials. Therefore, this investigation selected large round baler and typical forage grass alfalfa for the rotary compression tests. The aim is to establish compression model and stress relaxation model and study the effect of moisture content, feeding speed, and steel roll speed on maximum pressure, stress relaxation time, and equilibrium stress. Further, this then provides the theoretical basis and technical support for the analysis of the rotary compression mechanism and the optimization of the baling process.

EXPERIMENTAL

Materials

Alfalfa straw was used as the experimental material. It was harvested in the region of Hohhot (40°31′ N, 110°46′ E) in the Inner Mongolia Automous Region of China. It can be used as a high quality animal feed and has been grown in large scale in Northwestern China to mitigate sand erosion. Alfalfa is a perennial leguminous forage with high straw quality. Its crops can be harvested two to three times per year (Zhou 2017). The moisture content of raw alfalfa material used in this study was 30%, and the average straw length was about 80 cm. The moisture content was adjusted to 18%, 21%, and 24% *via* air-drying. Whole uncrushed stems were used in the experiments. The moisture content of the material was determined in accordance to the ASABE S358.2 (2008) standard.

Orthogonal Experimental Design

The moisture content of alfalfa straw, feeding speed, and steel roll speed were selected as experimental factors, and the maximum compression pressure, stress relaxation time, and equilibrium stress were used as indices. The experiment was designed according to orthogonal tables of three factors and three levels L_9 (3). All the factors and levels are shown in Table 1. The width of the material paved on the belt conveyor was 1 m and the density was 3 $kg \cdot m^{-2}$. The material was evenly fed to the pickup, and the roll's deformation data was measured at 0.5-s intervals. After feeding, the bales continued to run in the chamber for 170 s to detect the stress relaxation state of the bale. The determination time of the stress relaxation was determined by the results of a pre-experimental analysis and related literature (Zhao 2010). Approximately 330 kg of alfalfa straw was fed into the chamber to produce each bale. Each test was repeated three times and the result was taken average value.

Table 1. Factors of Levels by Orthogonal Experiments

Factor Level	Moisture Content of alfalfa straw A / (%)	Feeding speed B/(m·s-1)	Steel Roll Speed C/(r·min^{-1})
1	18	1.11	106
2	21	1.39	126
3	24	1.67	146

Methods

The rotary compression were performed using a round baler rotary compression test platform, which consisted of a steel-roll round baler (Model 9YG-1.3; HulunBuirMengTuo Farm Machinery Technology Co., Ltd; HulunBuir, China), belt conveyor, and power transmission system. An illustration is shown in Fig. 1:

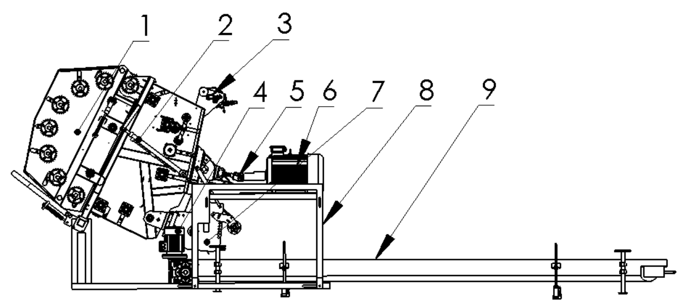

Fig. 1. Illustration of the rotary compression test platform for the round baler: 1 - Drive sprocket; 2 – rear door; 3 - chamber; 4 - hydraulic system; 5 - bale rope mechanism; 6 - conveyor motor; 7 - universal coupling; 8 - round baler motor; 9 - pickup; 10 - round baler support frame; and 11 - belt conveyor

As shown in Fig. 1, the rated speed of the steel-roll round baler was 126 r·min^{-1}, the quality of hay bales produced by the round baler was less than 350 kg, the diameter of the bales was 1.3 m, the length of the bales was 1.5 m, and the production efficiency of the round baler was 12~30 bales per hour. The round baler was driven by a 30 kW motor. A belt conveyor driven by a 4 kW motor was used to transport material to the pickup. Two frequency converters was used to control the speed of conveyor belt motor and round baler motor respectively to realize the parameter adjustment of feed quantity and steel roll speed.

To obtain the radial stress of the steel roll during the rotary compression of the bale, a strain gauge was arranged on the steel roll's surface. The deformation data were obtained by a wireless resistance strainer, and thus, the radial stress of the steel roll was obtained by an ANSYS commercial software (ANSYS, Inc., Apex, NC, USA) simulation analysis. According to Newton's Third Law, the radial stress of the steel roll to the bale is the same as the radial stress of bale to the steel roll.

The structure of the steel baling roll is shown in Fig. 2. There are 5 strip support plates inside the steel roll that are welded to the edge roller plates. The whole steel roll is driven by a sprocket drive.

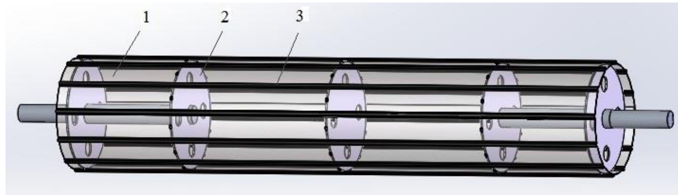

Fig. 2. Structure schematic of steel roll: 1 - 12-edge roller plate; 2 - convex edge; 3 - strip support plate

The wireless resistive strain gauge (Model SG404; Beijing BeeTech Inc., Beijing, China) consisted of a BA120-1AA-Q30P300 strain gauge, a SG404 wireless strain node, and a BS903 wireless gateway. The resistance value of the strain gauge was 120 Ω. The metering range of the SG404 wireless strain node was -15000 με to 15000 με. The precision of the SG404 wireless strain node was ± 0.2%. The strain gauge parallel to the axis was pasted to a convex edge of the tested steel roll at a distance from the middle strip support plate 216.5 mm, and the strain gauge is pasted along the axial direction. The wireless strain node, connected to the strain gauges, was attached to the inside of the steel roll via a magnetic seat. The wireless gateway was used to receive the transmitted strain data; the wireless gateway was interfaced with a laptop computer running BeeData software (V11.7; Beijing BeeTech Inc., Beijing, China) (Fig. 3). The raw experimental data was displayed and saved in the BeeData software, which was then analyzed using MATLAB 8.0 software (MathWorks, Natick, MA, USA). The data collection system for the baler is shown in Fig. 4.

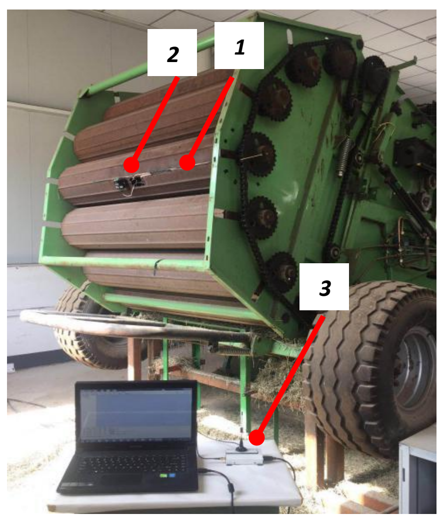

Fig. 3. Steel roll strain-measuring device: 1 - strain gauges; 2 - wireless strain node; and 3 - wireless gateway

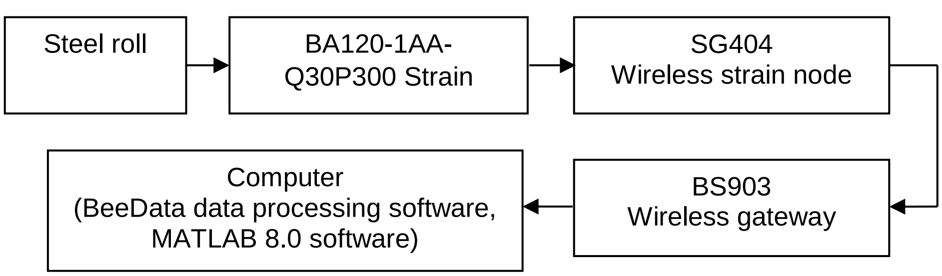

Fig. 4. Schematic of the experimental data collection system from the baler

The ANSYS simulation interface is shown in Fig. 5. The convex edge and half of the roller plates on both sides were regarded as continuous beam, and the five support plates were regarded as sliding hinge supports to define the model. The material attribute data were defined. The edge roller plates material was Q235A. The elastic modulus of Q235A was 2.1×105 MPa. The Poisson's ratio of Q235A was 0.3. The density of Q235A was 7850 kg·m^{-3}. The size of the continuous beam was 1486 mm × 74.5 mm × 6 mm. A uniform stress load was applied. The load form of the applied load was consistent with the load form of the steel roll in the actual rotary compression process. The strain result was obtained. The load was constantly adjusted until the simulated and actual deformation values were within statistical error of the actual value. Finally, the radial stress of the steel roll in the rotary compression (*i.e.*, the radial stress of the bales) can be calculated,

$$\sigma(t) = \frac{N(t)}{A} \times 10^3 \tag{1}$$

where σ(t) is the radial stress of steel roll (kPa) at time t (s), $N(t)$ is the radial force of steel roll (N) at time t, and A is the area of continuous beam (mm^2).

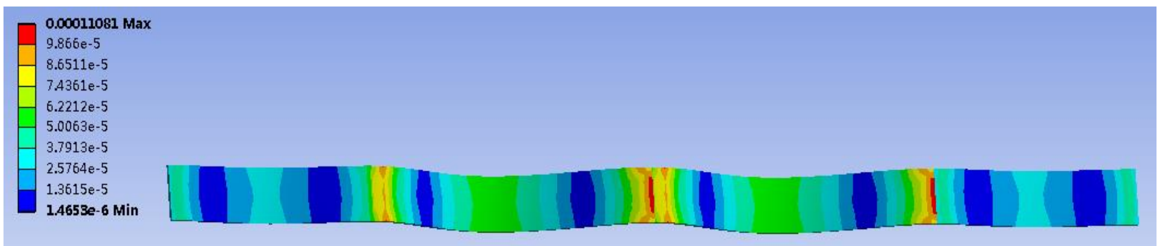

Fig. 5. ANSYS simulation interface

The collected deformation data were analyzed using MATLAB 8.0 software, and the outlier values were identified and excluded. The average value of each 5 s of data was taken as the measured deformation of the steel roll. Finally, all deformation data were transformed into radial stress by ANSYS commercial software (ANSYS, Inc., Apex, NC, USA), and the change in the radial stress of the bale of each test was calculated.

Data Analysis

Statistical analysis of orthogonal experimental results was performed using SPSS software (IBM, version 25.0, Chicago, IL, USA). The experimental data of each combination were all fitted to three compression models and a generalized Maxwell model using Origin 7.5 software (OriginLab), which can help design the most energy-efficient baler. The coefficient of determination (R^2) was used to evaluate the model fit to the experimental data.

Viswanathan and Gothandapani (1999) have studied the pressure-density relationship of compressed coir pith. They have come up with the second order polynomial equation.

$$P = c_1 + c_2\rho + c_3\rho^2 \tag{2}$$

where c_1, c_2, and c_3 are model constants.

Jones (1960) expressed the density-pressure data of compacted metal powder in the form of the following equation,

$$\ln(\rho) = m \ln(P) + b \tag{3}$$

where, m and b are model constants.

Faborode and O'Callaghan (1986) have studied compression behaviors of fibrous agricultural materials and have proposed the following equation to represent pressure during the compression process in terms of the initial density and compression ratio.

$$P = A[e^{B(\frac{\rho_0}{\rho}-1)} - 1] \tag{4}$$

where ρ_0 is the initial density of materials, kg/m^3, and A and B are model constants.

The simulation of the stress relaxation process is generally based on the generalized Maxwell model (Mohsenin and Zaske 1976; Shaw and Tabil 2007), which can be expressed with the following equation,

$$\sigma(t) = \sum_{i=1}^{n} A_i e^{\frac{-t}{T_i}} + \sigma_e \qquad (T_i = \eta_i / E_i) \tag{5}$$

where, $\sigma(t)$ is the stress during relaxation process (kPa), A_i is the maximum stress for the ith Maxwell element (kPa), T_i is the stress relaxation time for the ith Maxwell element (s), η_i is the viscosity coefficient for the ith Maxwell element, E_i is the elastic modulus for the ith Maxwell element, and n is the number of the Maxwell elements in the n-order Maxwell model. σ_e is the equilibrium stress in the model (kPa).

RESULTS AND DISCUSSION

Alfalfa Compression Curve

Graphs of the radial stress versus time of each material property and condition combinations, based on the measured data, were generated in MATLAB 8.0 software. Figure 6 shows a typical characteristic curve of compression. The compression curves can be divided into three stages. These were designated as a filling stage (Line AB), a rolling stage (line BC), and a stress relaxation stage (line CD). In the filling stage, the material accumulates and rolls continuously in the chamber with the rotation of the steel rollers. The steel roll provided friction to the bale and did not generate the force for extrusion.

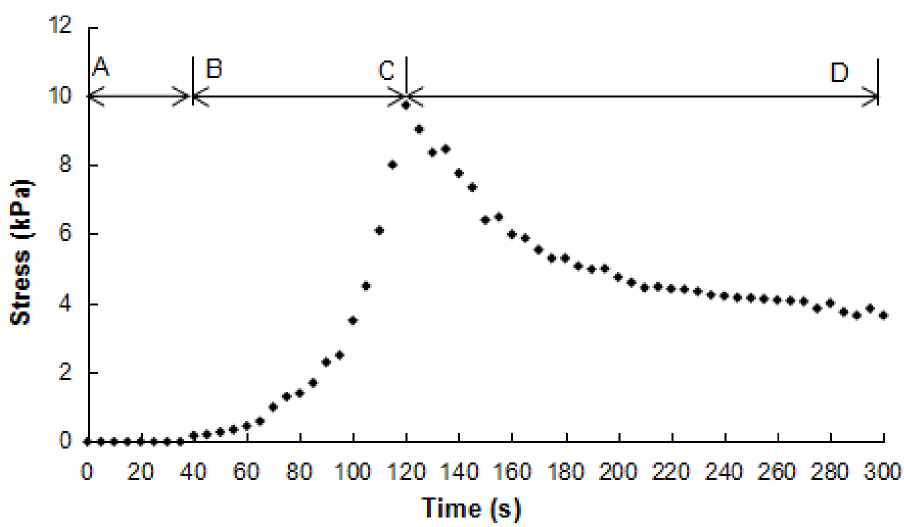

Fig. 6. Typical compression characteristic curve with 21% moisture content alfalfa at 1.11m/s feeding speed, 126r/min steel roll speed

The grass material mainly overcomes the air gap between each other and moves toward the center of the chamber. The grass material was loose and was not deformed in the initial stage. In the stage denoted by line BC, the material was extruded and deformed by the radial force of the steel roll. The density of the bale continuously increased as the radial force increased; finally, the bale was formed. Comprehensive deformation occurred between the grass materials, including elastic, plastic, and viscous deformation. The straw fed into the baler was stopped at 115 s, and the bale continued to operate in the chamber. Five seconds after the end of feeding, the stress value still increased. The bale was still in the rolling stage. In the stage denoted by line CD, The deformation of the bales was constant while the stresses continuously decreased. This defines a typical stress relaxation process.

Maximum compression pressure

The effects of moisture content, feeding speed and steel roll speed on maximum compression pressure were obtained by variance analysis (ANOVA), as shown in Table 2. The result showed that the moisture content and feeding speed had great influence on the maximum compression pressure, while the steel roll speed had no significant effect on the maximum compression pressure. F-value can evaluate the contribution rate of each factor to evaluation index. Table 2 showed that the order of the F-value from large to small was as follows: moisture content > feeding speed > steel roll speed. Since the maximum compression pressure was positively related to the power consumption, the moisture content of alfalfa should be strictly controlled during baling process. The feeding speed should be properly controlled, and the relationship between the feeding speed and the steel roll speed should be coordinated.

Table 2. ANOVA Results for Maximum Compression Force

Source of variation	df	Sum of squares	F	F_α
Moisture content	2	187286.524	136.337*	19.000
Feeding speed	2	52770.046	38.415*	19.000
Steel roll speed	2	1615.638	1.176	19.000
Error	2	1373.70		

Note：* means significant

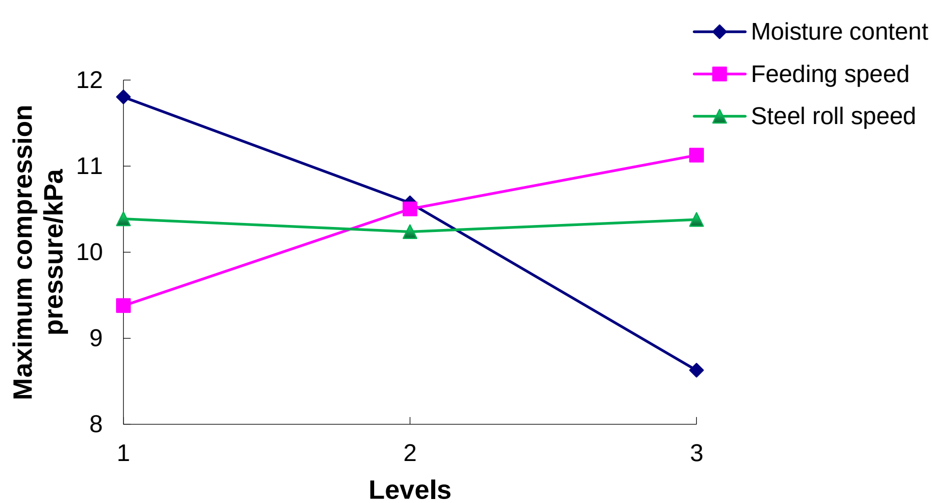

Fig. 7. The influences of process parameters on the maximum pressure

Through an orthogonal experiment, the influences of process parameters on the maximum pressure were obtained, as shown in Fig. 7. As moisture content increased, the maximum compression pressure decreased. This is because the increase in moisture content reduces the frictional force between the alfalfa straw and thus is easy to be compressed. The maximum compression pressure increased with increasing feeding speed. The increase of feeding speed makes the contact area of alfalfa straw larger. The friction between the materials and the mechanical strength of alfalfa increase, and thus it is not easy to be compressed. There were no significant differences in the maximum compression force at different speed roll speed.

Compression models

The relationship between pressure and density of alfalfa during compression stage of the tests (*i.e.* until maximum loading was achieved) were fitted to compression models. The Viswanathan and Gothandapani model describes the relationship of compact density to pressure using a second order equation. The R^2 value of each test combinations resulted in a fitted Viswanathan and Gothandapani model were greater than 0.96. Figure 8 shows a sample relationship between the pressure and compact density. The values of coefficient c_1 in Eq. 1 range from 1.25 to 7.51, values for c_2 range from -0.22 to -0.04, and values for c_3 range from 9.9×10^{-4} to 1.4×10^{-3}. The values of the coefficients in the equations did not follow any specific trend with the moisture contend, the feeding speed and the steel roll speed. Also, no relationships was proposed by the previous researchers.

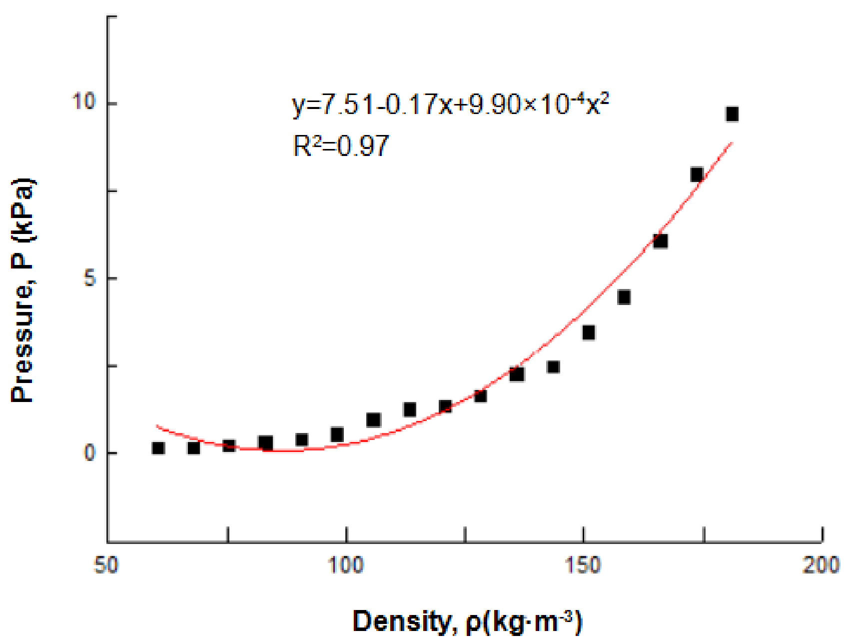

Fig. 8. Fitted Viswanathan and Gothandapani model to compression data for 21% moisture content alfalfa at 1.11m/s feeding speed and 126r/min steel roll speed

The Jones Model describes the compression of materials through the linear relationship of the natural logarithm of both pressure and density. The R^2 value of each test combinations resulted in a fitted Viswanathan and Gothandapani model were above 0.95. The values of the slope, m, for the model indicates the compressibility of the material.

The slope had an average value of 0.24. The value of *b* of the Jones model was relatively constant for all tests at an average of 4.33.

The Faborode and O'Callaghan model uses an exponential compression ratio equation to explain the compression behaviors of fibrous agricultural materials. The higher the compression ratio, the higher the compression pressure. Fitting the model to the experimental data yield values for A ranging from 0.003 to 0.23 and values for B ranging from -13.37 to -7.27. The R^2 values of each combination were above 0.98, indicating a good fit of the model to the experimental data.

Stress Relaxation Characteristics

The data in stress relaxation stage of alfalfa were fitted to the generalized Maxwell model by the residual method (Fang and Zhang 2018). A typical stress relaxation curve of the alfalfa with 21% moisture content alfalfa at 1.11 m/s feeding speed and 126 r/min steel roll speed is given in Fig. 9. There was a parallel spring in the model, whose stress did not relax, which is called the equilibrium stress. The stress of the residual curve was close to zero after two residuals which was represented by two exponential terms. In all cases, the stress relaxation model for alfalfa can be described by a generalized Maxwell model composed of two Maxwell elements and the equilibrium stress, and expressed as:

$$\sigma(t) = A_1 e^{-t/\tau_1} + A_2 e^{-t/\tau_2} + \sigma_e \tag{6}$$

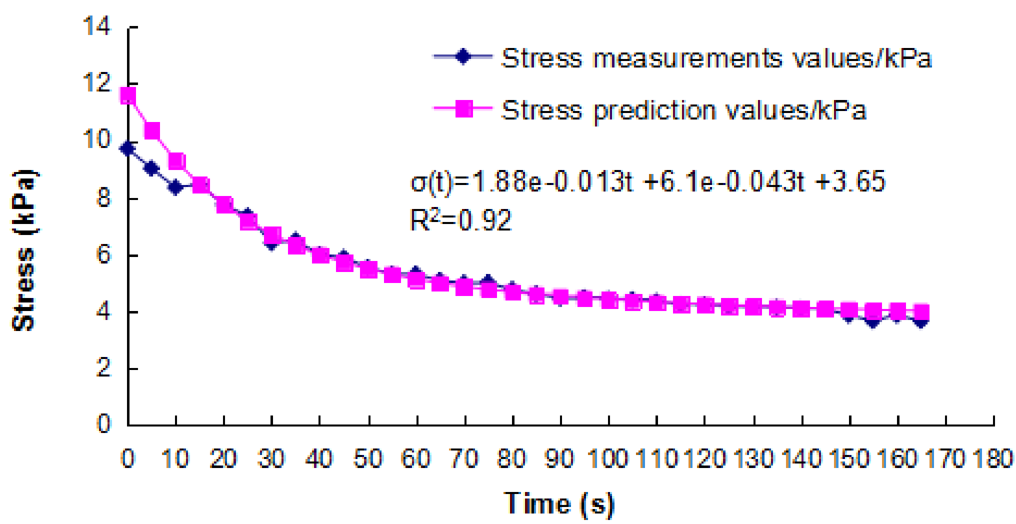

Fig. 9. Stress measurements and stress prediction values of 21% moisture content alfalfa at 1.11 m/s feeding speed and 126 r/min steel roll speed

The values of coefficients in Eq (5) are given in Table 3 for all test combinations. The smaller stress relaxation time in each stress relaxation model ranged from 23.3 s to 57.0 s, the larger stress relaxation time ranged from 45.4 s to 88.9 s, and the equilibrium stress ranged from 3.05 kPa to 5.84 kPa.

Table 3. Coefficients for the Stress Relaxation Character of Alfalfa of Each Material Property and Compression Condition Combination

No.	Moisture content	Feeding speed	Steel roll speed	Stress, kPa			Relaxation time, s		Coefficient of determination (R^2)
				A_1	A_2	σ_e	τ_1	τ_2	
1	1	1	1	4.67	1.5	5.83	37.01	88.92	0.94
2	1	2	2	4.42	1.9	5.78	57.03	78.65	0.90
3	1	3	3	4.75	2.61	5.84	52.01	67.43	0.91
4	2	1	2	6.1	1.88	3.65	23.26	76.92	0.92
5	2	2	3	6.12	1.33	4.25	44.07	69.44	0.91
6	2	3	1	3.36	3.5	5.24	27.11	61.78	0.93
7	3	1	3	2.52	2.43	3.05	34.27	45.43	0.95
8	3	2	1	3.04	1.6	4.76	37.04	50.89	0.89
9	3	3	2	3.52	2.89	4.59	39.24	45.77	0.92

The larger stress relaxation time in each stress relaxation model were considered in the analysis of the effects of moisture content, feeding speed and steel roll speed on stress relaxation time. The ANOVA result of the stress relaxation time and the equilibrium stress were shown in Table 4 and Table 5, respectively. The result showed that the moisture content, feeding speed, and steel roll speed all had great influence on the stress relaxation time and equilibrium stress. Table 4 showed that the order of the F-value from large to small was as follows: moisture content > feeding speed > steel roll speed. Table 5 showed that the order of the F-value from large to small was as follows: moisture content > feeding speed > steel roll speed.

Table 4. ANOVA results for stress relaxation time

Source of variation	df	Sum of squares	F	F_α
Moisture content	2	4.958	78.698*	19.000
Feeding speed	2	1.749	27.762*	19.000
Steel roll speed	2	1.254	19.905*	19.000
Error	2	0.06		

Note：*means significant

Table 5. ANOVA results for equilibrium stress

Source of variation	df	Sum of squares	F	F_α
Moisture content	2	4.958	78.698*	19.000
Feeding speed	2	1.749	27.762*	19.000
Steel roll speed	2	1.254	19.905*	19.000
Error	2	0.06		

Note：*means significant

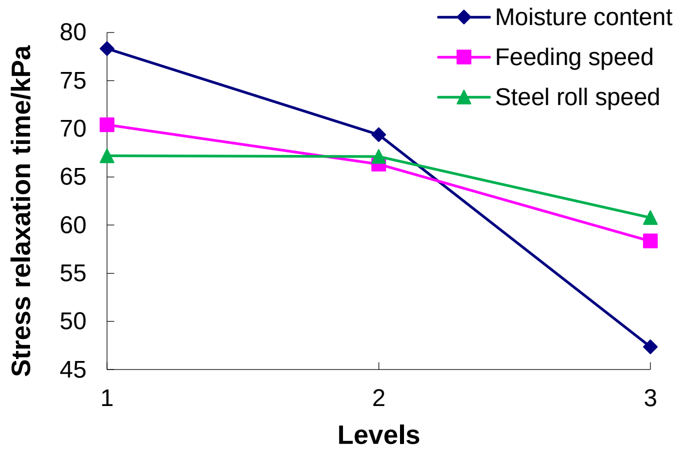

Fig. 10. The influences of process parameters on the stress relaxation time

Figure 10 shows the influences of the process parameters on the stress relaxation time. The stress relaxation time decreased with the increase of moisture content, feeding speed and steel roll speed. As moisture content increased, the viscosity coefficient of alfalfa drop rapidly resulted in a decrease in stress relaxation time. With higher feeding speed, the elastic modulus of the bale is greater and thus, the stress relaxation time is less. The increase of speed roll speed of can promote the flow of alfalfa straw in chamber, which accelerates the stress relaxation rate.

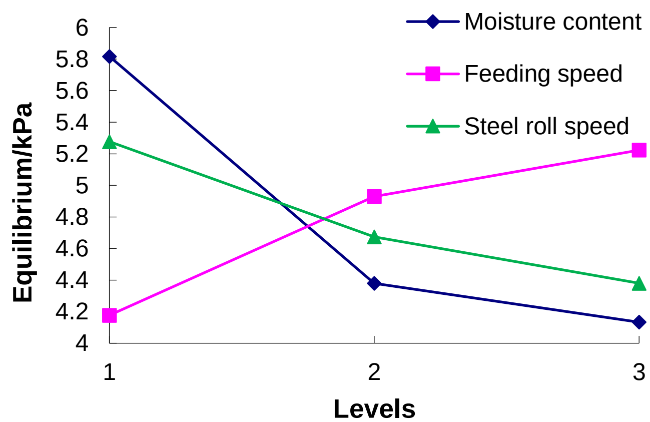

Fig. 11. The influences of process parameters on the equilibrium stress relaxation

Figure 11 shows the influences of the process parameters on the equilibrium stress. The equilibrium stress appeared to decrease with an increase in either moisture content or speed roll speed. This is because the viscosity of alfalfa decreased with the increase of moisture content. The rate of stress relaxation increases and the equilibrium stress decreases. The increase of steel roll speed is beneficial to the redistribution of alfalfa in chamber, thereby accelerating the release of the internal stress of the bale, and the equilibrium stress is reduced. The equilibrium elastic modulus increases with the increase of feeding speed. This reasonable as the higher the feeding speed, the thicker the alfalfa straw layer entering the chamber. The deformation of the rice straw is insufficient, and thus, a larger equilibrium stress.

The shorter stress relaxation time and the smaller the equilibrium stress are beneficial to reduce the spring back of the bale and increase the quality of the bale. Therefore, during the baling process, the higher moisture content and steel roller speed and the moderate feeding speed should be selected.

CONCLUSIONS

1. The Viswanathan and Gothandapani model, the Jones model, and the Faborode and O'Callaghan model all had a good fit for the experimental data, with the regression values (R^2 values) greater than 0.95. The stress relaxation model for alfalfa of each combination can be described by a generalized Maxwell model composed of two Maxwell elements and the equilibrium stress. The larger stress relaxation time ranged from 45.4 s to 88.9 s and the equilibrium stress ranged from 3.05 kPa and 5.84 kPa.
2. The order of contribution rate of each factor to maximum compression pressure, stress relaxation time and equilibrium stress were as follows: moisture content > feeding speed > steel roll speed.
3. The moisture content of the grass should be strictly controlled during the baling process. The higher moisture content and steel roller speed and the moderate feeding speed should be selected.

ACKNOWLEDGMENTS

This research was funded by the National Natural Science Foundation of China (Grant No. 61563042) and the Grassland Talents Modern Agriculture and Animal Husbandry Engineering New Technology R&D and Application Innovation Talent Team.

REFERENCES CITED

ASABE S358.2 (2008). "Moisture measurement—Forages," American Society of Agricultural and Biological Engineers, St. Joseph, MI, USA.

Adapa, P. K., Tabil, L. G., Schoenau, G. J., Crerar, B., and Sokhansanj, S. (2002). "Compression characteristics of fractionated alfalfa grinds," *Powder Handling and Processing* 14(4), 252-300. DOI: 10.13031/2013.23511

Adapa, P., Schoenau, G., Tabil, L., Sokhansanj, S., and Singh, A. (2005). "Compression of fractionated sun-cured and dehydrated alfalfa chops into cubes: Pressure and density models," *Canadian Biosystems Engineering* 47(3), 33-39. DOI: 10.1016/j.biortech.2005.11.032

Adapa, Tabil, and Schoenau. (2009). "Compaction characteristics of barley, canola, oat and wheat straw," *Biosystems Engineering* 104(3), 335-344. DOI: 10.1016/j.biosystemseng.2009.06.022

Faborode, M. O., and O'Callaghan, J. R. (1986). "Theoretical analysis of the compression of fibrous agricultural materials," *Journal of Agricultural Engineering Research* 35(3), 175-191. DOI: 10.1016/s0021-8634(86)80055-5

Fang, J., and Zhang, Y. (2018). "Stress relaxation behavior and modeling of alfalfa during rotary compression," *Transactions of the Chinese Society of Agricultural*

Engineering (Nongye Gongcheng Xuebao) 34(16), 50-56. DOI: 10.11975/j.issn.1002-6819.2018.16.007

Hu, J., and Lei, T. (2009). "Stress relaxation in straw molding," *BioResources* 4(3), 1158-1167. DOI: 10.15376/biores.4.3.1158-1167

Jones, W. (1960). *Fundamental Principles of Powder Metallurgy*, E. Arnold, London.

Lei, J. (2015). "Experiment on stress relaxation characteristics of intact rice straw during rotary compression," *Transactions of the Chinese Society of Agricultural Engineering (Nongye Gongcheng Xuebao)* 31(8), 76-83. DOI: 10.3969/j.issn.1002-6819.2015.08.012

Li, R. (2012). "Rheologic behavior of chopped corn stalks during rotary compression," *Transactions of the Chinese Society of Agricultural Engineering (Nongye Gongcheng Xuebao)* 28(18), 30-35. DOI: 10.3969/j.issn.1002-6819.2012.18.005

Mohsenin, and Zaske. (1976). "Stress relaxation and energy requirements in compaction of unconsolidated materials," *Journal of Agricultural Engineering Research* 21(2), 193-205.

Mani, S., Tabil, L. G., and Sokhansanj, S. (2002). "Compaction behavior of some biomass grinds," *AIC Paper* (02-305).

Mani, S., Tabil, L., and Sokhansanj. (2003). "An overview of compaction of biomass grinds," *Powder Handling and Processing* 15(3), 160-168.

Mani, Tabil, and Sokhansanj. (2006). "Specific energy requirement for compacting corn stover," *Bioresource Technology* 97(12), 1420-1426. DOI: 10.1016/j.biortech.2005.06.019

Sokhansanj, S., Mani, M., Stumborg, R., Samson, J., and Fenton. (2006). "Production and distribution of cereal straw on the Canadian prairies," *Canadian Biosystems Engineering / Le Genie Des Biosystems Au Canada*, 48, 3.39.

Shaw, M., and Tabil, L. (2007). "Compression and relaxation characteristics of selected biomass grinds," *2007 ASABE Annual International Meeting*, *Technical Papers*, 12. DOI: 10.13031/2013.23511

Watts, K. C., and Bilanski, W. K. (1991). "Stress relaxation of alfalfa under constant displacement," *Transactions of the ASAE* 34(6), 2491-2498. DOI: 10.13031/2013.31897

Viswanathan, R., and Gothandapani, L. (1999). "Pressure density relationships and stress relaxation characteristics of coir pith," *Journal of Agricultural Engineering Research* 73(3), 217-225. DOI: 10.1006/jaer.1998.0408

Yan, G. (2004). *Experimental Study on Fresh Material Compressing Process Stress Relaxation*, M.S. Thesis, Agriculture University of Inner Mongolia, Hohhot, China.

Zhao, H. (2010). *Study on Rotary Compression Characteristic of Chopped Corn Stalks*, M.S. Thesis, Agriculture University of Shandong, Shandong, China.

Zhou, Q. (2017). "Development situation and think of alfalfa forage grass industry in China," *Transactions of the China Dairy Cattle (Zhongguo Nainiu)* 5, 54-56. DOI: 10.19305/j.cnki.11-3009/s.2017.05.015

Article submitted: May 15, 2018; Peer review completed: August 10, 2018; Revised version received and accepted: March 23, 2019; Published: March 26, 2019.
DOI: 10.15376/biores.14.2.3860-3872